Extended Abstracts of the 2018 International Conference on Solid State Devices and Materials, Tokyo, 2018, pp827-828

First-Principles Based Ballistic Transport Simulation of Monolayer and Few-Layer InSe FETs

Pengying Chang[1], Xiaoyan Liu[1], Liu Fei[2] and Gang Du[1]
[1] Key Laboratory of Microelectronic Devices and Circuits (MOE), Institute of Microelectronics, Peking University, Beijing, 100871, China
[2] Center of Theoretical and Computational Physics, Department of Physics, University of Hong Kong, Hong Kong
Email: pychang@pku.edu.cn, xyliu@ime.pku.edu.cn

Abstract

In this work, ballistic performance of two-dimensional (2D) InSe n-type FETs as a function of layer number is investigated based on first-principles calculation using density functional theory (DFT) and top-of-the-barrier (ToB) transport model. DFT calculation suggests that the band structure, effective mass, and bandgap strongly depend on the layer number. Ballistic simulation reveals that the InSe FETs with reduced layer provide better performance, showing great potential for future high-performance CMOS application.

1. Introduction

Recently, 2D layered semiconductors have gained great attention to push further the limits of CMOS downscaling, due to their atomically thin structure and weak surface roughness scattering [1]. Among these 2D materials, few-layer InSe has recently exhibited attractive electronic properties with electron mobility of ~10^3cm^2/Vs at 300K [2]. The high mobility and bandgap of 1.4eV make InSe a perfect candidate for ultra-thin body FETs, offering similar gap as silicon, high mobility and 2D nature as graphene. However, theoretical study on transport performance of few-layer InSe FET are still highly required.

In this work, we present a DFT calculation and ballistic transport simulation of monolayer and few-layer InSe-based FETs, revealing the dependence of electronic structure and device performance on layer number or thickness.

2. Simulation Methods

The approach combines different levels of physical modeling. *i*) Band structure of few-layer InSe with atomic structure as shown in Fig.1 is calculated based on DFT using the VASP simulation package [3]. The Generalized Gradient Approximation is adopted for the exchange correlation potential, and spin-orbit interaction is excluded. The energy cutoff for the plane-wave basis is set to be 500eV. *k*-mesh for monolayer is $9\times9\times1$. Geometric optimization is completed until the maximum force is less than 0.001eV/Å. *ii*) Effective mass m^* is determined by the second derivative of a particular band dispersion: $1/m_{\alpha\beta}^*=(1/\hbar^2)(\partial^2E/\partial k_\alpha\partial k_\beta)$ at the band edge, and then the nonparabolicity coefficient α is extracted by fitting the E-k curves with a relation $E(1+\alpha E)=\hbar^2k^2/2m^*$[4]. *iii*) Electrostatic characteristic under quantum confinement is obtained by self-consistent calculation of the Schrödinger and Poisson equations based on effective mass approximation (EMA) for the double-gate (DG) InSe FETs, as shown in Fig.1. *iiii*) Electrical characteristic of InSe under the ballistic limits is simulated based on the ToB model [5], which is efficient and particularly useful to provide significant physical insight into the ballistic performance. To clarify the band structure effect, any scattering mechanisms and tunneling effects at the OFF-state bias are neglected, and the perfect electrostatic gate control over the channel is assumed.

3. Results and Discussions

Crystal structure For the monolayer (1L) InSe shown in Fig.1, the lattice constant, In-In distance, and Se-In-In-Se distance are 3.97, 2.94, and 5.29Å, respectively, which are in good agreement with the previous reports [6-9]. As thickness is necessary for the electrostatic calculation of 2D-based devices, we use 8.23Å as the thickness of 1L InSe, which corresponds to experimentally interlayer distance of InSe [10].

Band structure Fig.2 shows the electronic band structure in the Brillouin zone for 2D InSe with layer number L ranging from 1 to 16, as derived from DFT. It reveals that as L decreases, the conduction band minimum always locates at Γ point and shifts upwards to high energy; in contrast, the valence band maximum slightly shifts from the Γ point towards the K point. Thus a direct-to-indirect band transition occurs with decreasing L. Fig.3 shows the calculated bandgap of InSe versus the layer number. The bandgap decreases significantly from 1.64eV of the monolayer to 0.38eV of the 16-layer InSe. Furthermore, dependence of bandgap on layer number is consistent with previous reports [6-9, 11,12].

Electron effective mass Fig.4 shows the extracted electron effective mass m_e^* of monolayer and few-layer InSe along Γ-K and Γ-M directions. It reveals that m_e^* of InSe shows an isotropic feature, i.e., there is little difference between the Γ-K and Γ-M directions in contrast to MoS_2 and black phosphorus [11]. As L increase, m_e^* significantly decreases. Particularly, m_e^* of monolayer InSe is $0.18m_0$, which is consistent with previous calculations [6-9,11,12]. Then when InSe thickness is more than 6-layer, m_e^* gradually approaches the saturated value of $0.13m_0$, showing a good agreement with the experimental m_e^* value for 2DEG in InSe [13,14]. Fig.5 shows the lowest band dispersion of 1L InSe obtained from the DFT calculation and analytical EMA band without and with the nonparabolicity correction. Since the m_e^* is quite small and the parabolic dispersion persists up less than 200meV, which may cause serious inaccuracy of carrier density calculation in strong inversion due to the carrier occupation of higher energy band. Thus it is necessary to extract the nonparabolicity coefficients α. For InSe, α=0.45eV^{-1} is obtained, which is nearly a constant regardless of the layer number. Particularly, the nonparabolicity band matches well with DFT calculation up to 500meV.

Ballistic transport For DG InSe-based FETs shown in Fig.1, EOT=0.5nm and V_{DD}=0.5V are used. The gate work function is adjusted to obtain the same OFF-current I_{OFF} (0.1μA/μm) at V_G=0 and V_D=0.5V. Fig.6 shows the I_D-V_G characteristics, carrier injection velocity V_{INJ} and inversion sheet density N_S of few-layer InSe FETs, respectively. As the L decreases, the drain current significantly increases due to the change of m_e^*. Within the ballistic regime, the larger m_e^* implies a smaller V_{INJ} and a larger density-of-states (DOS). Therefore, the influence of larger m_e^* with reduced layer on DOS dominates and contributes to a larger N_S and then an increased current. In addition, simulation of MoS_2 FETs is also shown in Fig.6

as a benchmark. The ballistic performance of InSe-based FETs is significantly superior to that of MoS_2-based FETs. Particularly, I_{ON}= 2460μA/μm, and $I_{ON}/I_{OFF}>10^4$ at V_{DD}=0.5V for monolayer InSe FETs, satisfies the ITRS requirements for 2026 node for high-performance technology [15]. These results indicates that InSe FETs show great potential for future CMOS application.

4. Conclusions

This work reveals that the band structure, effective mass and ballistic performance of InSe FETs strongly depend on the layer number. Simulation results suggest that the layered InSe exhibits great potential for future CMOS applications by taking advantage of small effective mass and moderate bandgap.

Acknowledgements

This work is supported by the National Natural Science Foundation of China under Grant 61674008 and Grant 61421005.

References

[1] G. Fiori *et al.*, *Nature Nanotech.* **9**, 768 (2014).
[2] W. Feng *et al.*, *Adv. Mater.* **26**, 6587 (2014).
[3] G. Kresse and J. Furthmuller, *Phys. Rev. B* **54**, 11169 (1996).
[4] D. Esseni *et al.*, *Nanoscale MOS Transistors*, CUP.
[5] A. Rahman *et al.*, *IEEE Trans. Electron Dev.* **50**, 1853 (2003).
[6] E. Marin *et al.*, *IEEE Electron Dev. Letts.* 39, 626 (2018).
[7] C. Sun *et al.*, *Appl. Phys. Exp.* **9**, 035203 (2016).
[8] V. Zlyómi *et al.*, *Phys. Rev. B* **89**, 205416 (2014).
[9] S. Magorrian *et al.*, *Phys. Rev. B* **94**, 245431 (2016).
[10] G. Mudd *et al.*, *Adv. Mater.* **25**, 5714 (2013).
[11] Y.Ahn *et al.*, *IEEE Trans. Electron Dev.* **64**, 2129 (2017).
[12] G. Mudd *et al.*, *Scientific Reports* **6**, 39619 (2016).
[13] E. Kress Rogers *et al.*, *Solid-State Commu.* **44**, 379 (1982).
[14] D. Bandurin *et al.*, *Nature Nanotech.* **12**, 223 (2017).
[15] *International Technology Roadmap for Semiconductors*

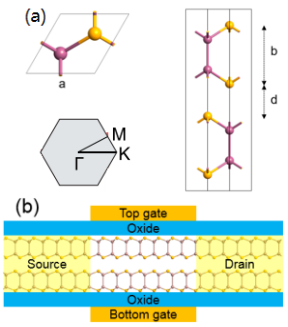

Fig.1 (a) Crystal structure of InSe. (b) Device structure of DG InSe FETs in the simulation.

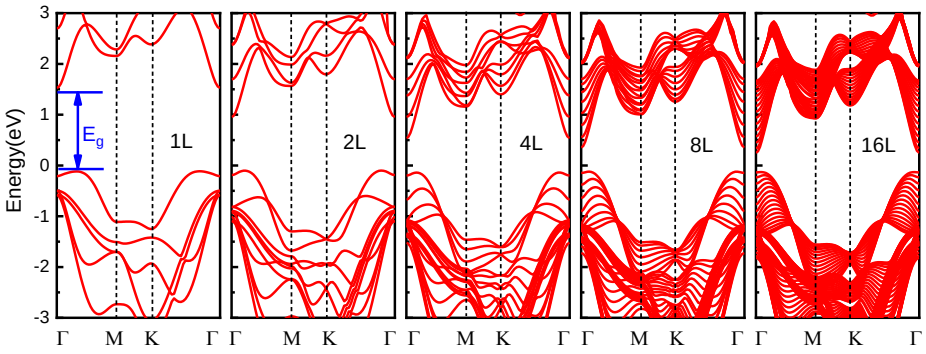

Fig.2 Band structure in the Brillouin zone for InSe with layer number L ranging from 1 to 16 derived from DFT. As L decreases, the conduction band minimum always locates at Γ point and shifts to high energy; in contrast, the valence band maximum slightly shifts from the Γ point towards the K point.

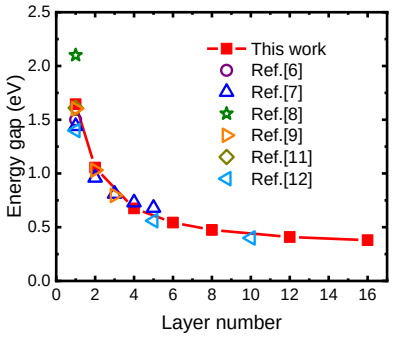

Fig.3 Bandgap of InSe versus layer number. Dependence of bandgap on layer number shows an excellent agreement with previous calculations [6-9,11,12].

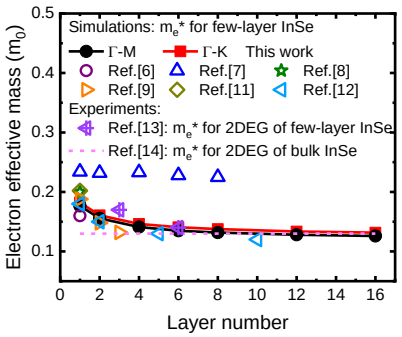

Fig.4 Electron effective mass m_e^* of few-layer InSe along Γ-K and Γ-M directions. Results from previous calculations and experiments are also shown [6-9,11-14].

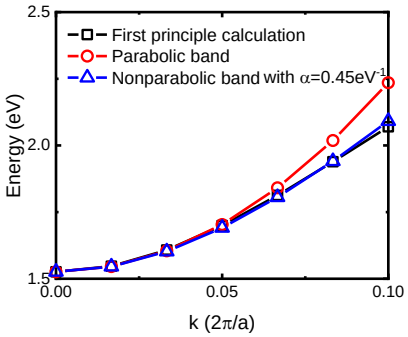

Fig.5 Lowest band dispersion of 1L InSe obtained from DFT calculation and analytical EMA band without and with the nonparabolicity correction.

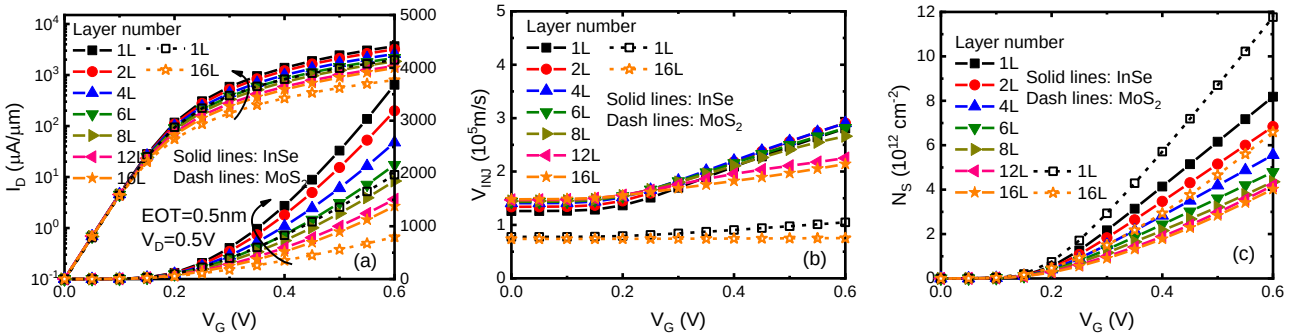

Fig.6 Characteristics of InSe FETs with layer number ranging from 1L to 16L. Simulation of MoS_2 FETs is also shown for a benchmark. (a) Ballistic I_D-V_G curves, (b) average injection velocity V_{INJ}, and (c) inversion sheet density N_S as a function of gate voltage V_G. It can be seen that as the L decreases, the drain current significantly increases, and InSe-based FETs is superior to MoS_2-based FETs.